

Phase diagram of a two-dimensional system which stabilizes Kagome lattice

Yu. D. Fomin ^{*1,2}

¹*Vereshchagin Institute of High Pressure Physics, Russian Academy of Sciences,
Kaluzhskoe shosse, 14, Troitsk, Moscow, 108840 Russia*

²*Moscow Institute of Physics and Technology (National Research University),
9 Institutskiy Lane, Dolgoprudny, Moscow region, 141701, Russia*

(Dated: June 2, 2020)

Phase diagram of a two-dimensional system with a potential which stabilizes Kagome lattice is calculated. It is shown that this system demonstrate a set of crystalline and the regions of stability of these phases are calculated. The scenarios of melting of triangular and square crystals of the system are determined.

PACS numbers: 61.20.Gy, 61.20.Ne

INTRODUCTION

Two-dimensional (2D) systems are of great interest for many fundamental and technological issues. They demonstrate some unusual features which make them strongly different from the three-dimensional (3D) ones. First of all, 2D systems do not have a genuine crystalline phase. As it was pointed out by Pierls and Landau [1] and then by Mermin [2], 2D crystals do not have long-range translational order. The translational order in 2D crystals is quasi long-ranged, i.e. the correlation functions decay algebraically. At the same time the orientational ordering of 2D crystals is long-ranged one, like in the case of 3D space.

This difference between 2D and 3D crystals leads to difference in the melting mechanisms. While in 3D melting is the first order phase transition, at least three different scenarios of melting of 2d crystals are widely discussed at the moment (see Ref. [3] for review of the problem). First, a 2D crystal can melt via the first order phase transition, as a 3D crystals do. The second scenario is a so-called Berezinskii-Kosterlitz-Thouless-Halperin-Nelson-Young (BKTHNY) melting [4–10]. In this scenario, melting proceeds via two stages. At the first step the orientational order transforms from long-range to quasi-long range, while the translational order becomes short range. It results in a phase which is neither solid, not isotropic liquid, since it demonstrates orientational ordering. This phase is called hexatic phase. At the second step of the melting process the hexatic phase loses the quasi-long-range orientational order and transforms into isotropic liquid. Importantly, both transitions in BKTHNY scenario are continuous infinite order transitions, i.e., all derivatives of the free energy are continuous at these transitions. Finally, one more scenario was proposed recently [11–13]. According to this scenario, melting of a 2D crystal proceeds via two transitions, but

while the transition from crystal to hexatic phase is a continuous transitions, the hexatic phase transforms into the isotropic liquid by the first order phase transition. Below we refer to this melting scenario as 'the third scenario'.

From the discussion above we see that melting of 2D crystals is a complex problem. At the same time the variability of crystalline structures in 2D space is much lesser than in 3D one: until recently it was supposed that 2D systems form a triangular crystalline structure only. The first study which attracted a lot of attention to formation of other type of crystalline structures in 2D space is the discovery of graphene [14]. Later on more complex structures were discovered in 2D and quasi-2D systems, for instance, square ice is formed when water is confined between two graphene planes [15], the square phase of 2D iron was discovered in a slit pore with graphene walls [16]. Many complex structures were observed in a system of colloidal particles in a magnetic field in the work [17]. However, up to now experimental observation of non-triangular 2D crystals is rather rare.

Surprisingly, many 2D systems which demonstrate non-triangular crystalline structures are obtained in computer simulation. The publications which report different types of crystalline and quasi-crystalline structures are numerous (see, for instance, [18–31] and references therein). Because of this one can expect that further experimental studies will led us to find more experimental 2D systems with complex phases.

A particular class of the models, which can demonstrate complex phase diagrams in the so-called 'core-softened systems', which are characterized by softening of the repulsive part of the interaction potential [32]. Depending on the shape of the potential core-softened systems can demonstrate complex phase diagrams (see Ref. [33] for review of the works on the phase diagrams of the core-softened systems). In our recent work a model core-softened system (Repulsive Shoulder System (RSS)) was

*Corresponding author: fomin314@mail.ru

proposed [34]

$$U(r)/\varepsilon = \left(\frac{d}{r}\right)^n + 0.5(1 - \tanh(k(r - \sigma))), \quad (1)$$

where $n = 14$, $k = 10$ and the parameter σ determines the width of the repulsive shoulder of the potential. The phase diagram of RSS in both 3D and 2D was studied (see [34–38] for 3D and [21–25] for the 2D phase diagrams). It was shown that in both 3D and 2D this system is characterized by very complex phase diagrams. In particular, in 2D case the system with $\sigma_1/\sigma = 1.35$ demonstrates a square crystal and a dodecagonal quasicrystalline phase [25].

A generalization of this system was proposed in Ref. [39]. By adding an attractive well to the potential (SRS - attractive well system - SRS-AW) we obtained a system with a potential with both repulsive step and attractive well:

$$U(r)/\varepsilon = \left(\frac{d}{r}\right)^n + \sum_{i=1}^2 (1 - \tanh(k_i(r - \sigma_i))). \quad (2)$$

In Refs. [39–42] we investigated the phase diagram of 3D SRS-AW system at different parameters of the potential.

The results of exploration of both SRS and SRS-AW systems showed that the phase diagrams of these systems are very sensitive to the parameters of the potential. Because of this other groups of researchers decided to use this potential to an inverse problem: given a particular structure they aim find parameters of SRS-AW potential which can stabilize it. In Ref. [43] a method to solve this problem was proposed. The authors proposed a scheme to compare the chemical potentials of different crystalline structures at zero temperature and given pressure and employed this scheme to find a potential (not of SRS-AW form) which stabilize a diamond structure. The same method was applied to the SRS-AW potential to stabilize different 3D and 2D structures in the works [44–46]. In particular, in Ref. [46] a parameterizations of the SRS-AW potential which stabilizes the Kagome lattice was proposed. Later on the properties of this particular system were investigated in Ref. [47]. All phases presented in the system were identified. However, the complete phase diagram of has not been constructed.

The goal of the present paper is to calculate the phase diagram of 2D SRS-AW system with the parameters which stabilize Kagome lattice. We find all structures existing in the system and calculate the regions of their stability in the density-temperature plane. We also discuss the scenarios of melting of the low-density triangular phase and the square phase of the system.

A	0.01978
n	5.49978
λ_1	-0.06066
k_1	2.53278
d_1	1.94071
λ_2	1.06271
k_2	1.73321
d_2	1.04372
r_c	3.0
P	0.007379
Q	0.04986
R	-0.085054

TABLE I: The potential parameters 3 used in the present study.

SYSTEMS AND METHODS

In this work we investigate the SRS-AW system (Eq. 2) with parametrization which stabilizes Kagome lattice [46]. In order to employ this parametrization, we rewrite the potential in the form of Ref. [46]:

$$U(r)/\varepsilon = A \left(\frac{\sigma}{r}\right)^n + \sum_{i=1}^2 \lambda_i (1 - \tanh(k_i(r/\sigma - d_i))) + U_{shift} \quad (3)$$

where $U_{shift} = Pr^2 + Qr + R$ is used to make both the potential and its first and second derivatives continuous at cut-off distance r_c . The parameters of the potential are given in Table I. The parameters σ and ε are used as the units of length and energy. All other quantities are expressed basing on these parameters. Only these dimensionless units are used throughout the paper.

We study the behavior of the system by means of molecular dynamics method. The system is simulated in a rectangular (or square depending on the phase simulated) box with periodic boundary conditions. We follow the same methodology that was used in Refs. [20, 48], i.e. firstly we study a small system of 4000 particles in a wide range of densities in order to get a rough estimation of the phase diagram. After that we simulate a larger system of 20000 particles in order to establish the melting scenarios of the low-density triangular phase and 22500 particles for the square phase. In all cases the system was simulated for $5 \cdot 10^7$ steps with the time step $dt = 0.001$. First $2 \cdot 10^7$ steps were discarded from the analysis and used for equilibration of the system. At the last $3 \cdot 10^7$ the properties of the system were calculated. We calculated the equations of state (EOS), i.e. the dependence of pressure on density at fixed temperature. The structure of the system was probed by radial distribution functions (RDFs) $g(r)$ and diffraction patterns (DP). The latter were calculated as

$$S(\mathbf{k}) = \left\langle \frac{1}{N} \left(\sum_i^N \cos(\mathbf{k}\mathbf{r}_i) \right)^2 + \left(\sum_i^N \sin(\mathbf{k}\mathbf{r}_i) \right)^2 \right\rangle.$$

RDFs and DPs give enough information to find out the structure of the system. However, they do not allow to establish the melting scenarios. In the present work we combine several methods to make a justified conclusion on the melting scenario. Firstly, we monitor the EOS of the system. If a first order transition takes place in the system, the EOS demonstrates a Mayer-Wood loop. Indeed, such a loop can appear even in the case of the second order phase transition [49]. However, we are not aware of any melting scenario which involves a second order transition. The BKT-type transitions which appear in BKTHNY and in the third scenarios are of infinite order, and no loop on the equation of state can appear in this case. Because of this we consider the presence of a loop as an evidence of the presence of the first order phase transition [48].

We also analyze the orientational and translational order parameters of the system. The local orientational order parameter (OOP) is defined as [8, 9, 50, 51]:

$$\psi_6(\mathbf{r}_i) = \frac{1}{n(i)} \sum_{j=1}^{n(i)} e^{in\theta_{ij}}, \quad (4)$$

where θ_{ij} is the angle of the vector between particles i and j with respect to the reference axis. The sum over j counts $n(i)$ nearest-neighbors of i . Voronoi construction is used to find the nearest neighbors of a particle.

The global OOP is obtained by averaging of the local OOP over the whole system:

$$\Psi_6 = \frac{1}{N} \left\langle \left| \sum_i \psi_6(\mathbf{r}_i) \right| \right\rangle. \quad (5)$$

The translational order parameter is defined as [8, 9, 50, 51]:

$$\Psi_T = \frac{1}{N} \left\langle \left| \sum_i e^{i\mathbf{G}\mathbf{r}_i} \right| \right\rangle, \quad (6)$$

where \mathbf{r}_i is the position of i -th particle and \mathbf{G} is the reciprocal-lattice vector of the first shell of the crystal lattice.

Further analysis of ordering in the system is undertaken by calculations of correlation functions of OOP and TOP. The orientational correlation function (OCF) is calculated as:

$$g_6(r) = \frac{\langle \Psi_6(\mathbf{r}) \Psi_6^*(\mathbf{0}) \rangle}{g(r)}, \quad (7)$$

where $g(r) = \langle \delta(\mathbf{r}_i) \delta(\mathbf{r}_j) \rangle$ is RDF of the system. In the case of crystal the OCF has a flat shape, i.e. it does not decay at the scale of the sample. In the hexatic phase the long-range behavior of $g_6(r)$ has the form $g_6(r) \propto$

$r^{-\eta_6}$ with $\eta_6 \leq \frac{1}{4}$ [8, 9]. In isotropic liquid OCF decays exponentially.

The translational correlation function (TCF) is defined as

$$g_T(r) = \frac{\langle \exp(i\mathbf{G}(\mathbf{r}_i - \mathbf{r}_j)) \rangle}{g(r)}, \quad (8)$$

where $r = |\mathbf{r}_i - \mathbf{r}_j|$. In the solid phase the long-range behavior of $G_T(r)$ has the form $g_T(r) \propto r^{-\eta_T}$ with $\eta_T \leq \frac{1}{3}$, i.e. it decays algebraically [8, 9]. In the hexatic phase and isotropic liquid g_T decays exponentially, i.e. these phases demonstrate short-range translational order only.

The combination of EOS with analysis of order parameters and their correlation functions allows to distinguish between the three melting scenarios unambiguously.

RESULTS AND DISCUSSION

In this section we calculate the phase diagram of the system under investigation. As it has been mentioned above, all phases presented in the system have been identified in Ref. [47], but the authors have not calculated the complete regions of stability of these phases. Going from low density to high one, one observes the following sequence of phases: fluid \rightarrow hexatic \rightarrow low density triangular solid \rightarrow hexatic \rightarrow square solid (possibly with the advent of tetratic phase) \rightarrow dimers (or pairs in terms of Ref. [47]) \rightarrow oblique crystal (stripe phase) \rightarrow Kagome lattice \rightarrow high density triangular crystal. Fig. 1 shows the whole phase diagram obtained in the present study. Below we discuss the properties of all phases and the transition lines in more detail.

The first crystal structure which appears in the system is the low-density triangular phase. As the density increases it transforms into the square crystal. We will discuss the properties of these phases in more detail below.

The next structure after the square crystal is a phase of dimers (or pairs). The mechanisms of formation of this phase are discussed in Ref. [47]. It is also shown in the same publication that the centers of mass of the dimers form a stretched hexagonal lattice. Fig. 2 (a) and (b) show a snapshot of the phase of dimers and a diffraction pattern of the same phase. The diffraction pattern shows clear hexagonal features, which confirms the conclusions of Ref. [47].

When the density increases the phase of dimers transforms into stripe phase. The structure of the stripe phase was identified in our recent publication [53]: the stripe phase is an oblique crystal. The primitive vectors of this phase are of different length and the angle between these vectors is about 40 degrees. The mechanisms of transformation of the dimers into stripes were revealed in Ref. [47]. Since dimers and stripes were widely discussed in the recent papers [47, 53] we do not discuss these phases

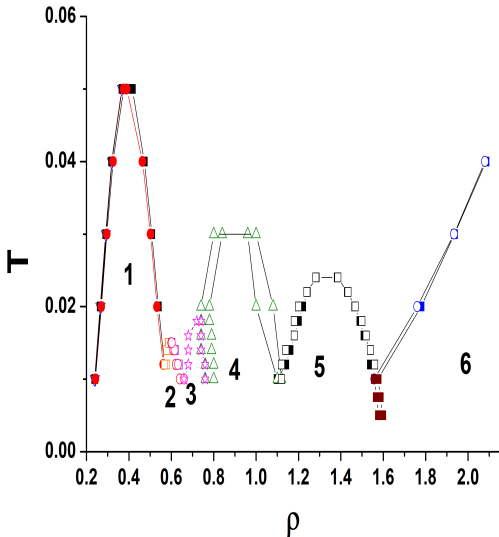


FIG. 1: Phase diagram of the system. The phases are denoted by numbers. 1 - low-density triangular phase, 2 - square phase, 3 - dimers (pairs), 4 - oblique crystal (stripe phase), 5 - Kagome lattice, 6 - high-density triangular crystal.

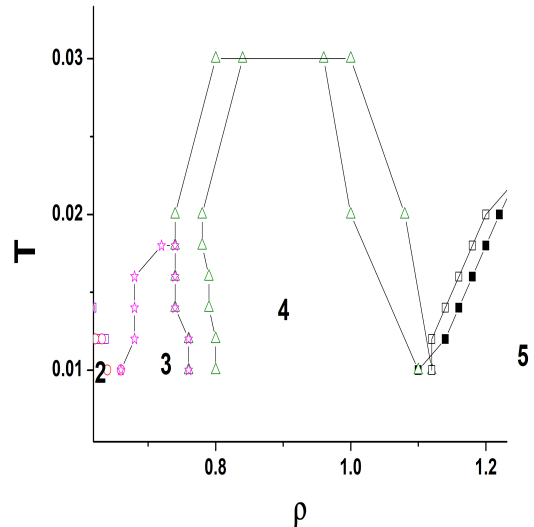


FIG. 3: The phase diagram of the system in the vicinity of the phase of dimers (3) and stripes (4).

in detail here, but give the limits of stability of these phases only (Fig. 3). Interestingly, the phase of dimers is stable at low temperatures only. The oblique crystal is stable up to much higher temperatures. Because of this it coexists with dimers at low temperature and with liquid at the higher one.

At higher densities the stripe phase transforms into Kagome lattice which on further densification experiences a transition into high-density triangular phase. The Kagome phase is stable in a rather wide range of densities. Although Kagome lattice is very unusual for one component systems, it can be observed in complex colloidal systems [54]. In this respect it is of special interest to find out the mechanisms responsible for the formation of the Kagome lattice. However, this problem is far from being solved.

Having identified all structures in the system, we turn to more detailed investigation of melting lines of the low-density triangular and square phases. First we consider the low-density triangular phase. This phase is studied with the system of 20000 particles. Fig. 4 shows the equation of state, TCF and OCF of this system at the low-density branch of the melting line at $T = 0.02$. One can see that the EOS demonstrates a Mayer-Wood loop, i.e., first order transition takes place in the system. In order to distinguish between the first and the third scenarios we calculate the orientational and translational correlations functions. From these plots one can see that, if one goes from higher densities to the lower ones, the crystal loses its stability to the hexatic phase prior to the Mayer-Wood loop, i.e., there is a continuous transition from crystal to the hexatic phase, and, therefore, the

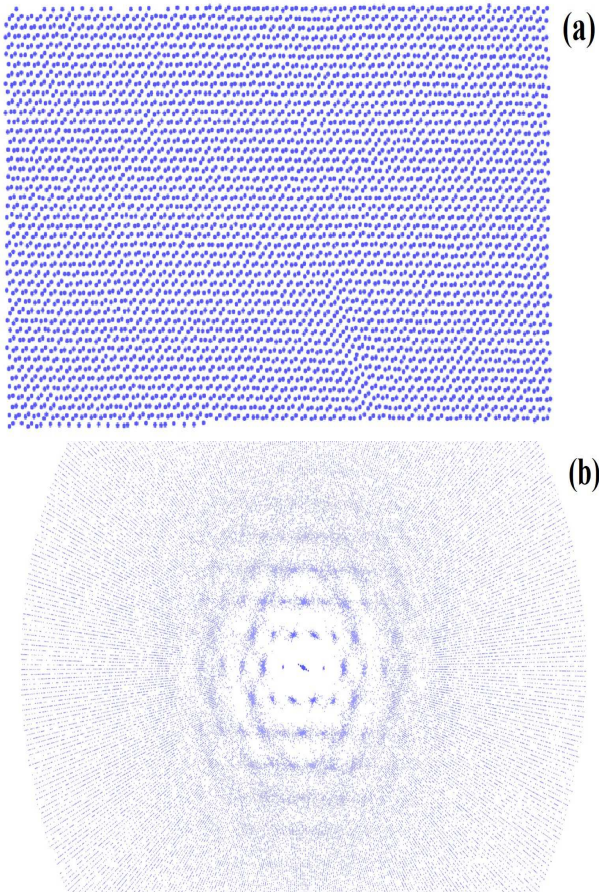


FIG. 2: (a) A snapshot of the system at $T = 0.012$ and $\rho = 0.7$ (phase of dimers). (b) Diffraction pattern at the same point.

loop corresponds to the first-order transition between the hexatic phase and isotropic liquid. Therefore, the third scenario is realized in this case.

The behavior of the melting line at the high-density branch of the melting line of the low-density triangular crystal is different. In this case we do not observe the Mayer-Wood loop (Fig. 5), and therefore the melting appears via BKTHNY scenario. The limits of stability of the crystal and hexatic phase are calculated from the TCF and OCF functions.

The phase diagram in the vicinity of the low-density triangular phase is shown in Fig. 6.

In our previous publications we studied the Hertz system, which is characterized by the interaction potential $U(r) = \varepsilon(r - \sigma)^\alpha$, if $r < \sigma$ and zero otherwise. We found that in the case of $\alpha = 5/2$ there are two tricritical points on the melting line of the low-density triangular phase [20]. One of them is at the maximum of the melting line and another one is on the high-density branch. In the case of $\alpha = 7/2$ a single tricritical point at the low density branch is observed [48]. The low-density triangular phase of the RSS-AW system melts via the third scenario at the low-density branch and the BKTHNY scenario at the high-density branch. However, we do not find the second tricritical point in the RSS-AW system. Therefore, the melting behavior of the low-density triangular phase of SRR-AW system is similar, but not equivalent to the one of the Hertzian spheres with $\alpha = 5/2$.

The same calculations are performed for the square phase. A system of 22500 particles in a square box is used in this case. Fig. 7 shows the behavior of the system across the melting line of the square phase at $T = 0.012$. One can see that there is no Mayer-Wood loop on the equation of state. At the same time the g_{t-sq} and g_4 criteria give different transition points. Because of this we conclude that the system melts via BKTHNY scenario.

However, the high-density branch of the square crystal behaves differently (Fig. 8). First of all, there is a clear Mayer-Wood loop, therefore, first order phase transition takes place in the system. The limit of stability of the crystal with respect to the tetratic phase preempts the first order transition points, while the limit of stability of the tetratic phase with respect to the liquid obtained on the basis of OCF criterion is inside the loop. Therefore, the third scenario takes place in the system.

We conclude that the melting line of the square crystal consists of BKTHNY part at the low-density branch and the third scenario at the high density one. The tricritical point is at the maximum of the melting line. The part of the phase diagram in the vicinity of the square crystal is shown in Fig. 9.

CONCLUSIONS

In conclusion, we have studied the phase diagram of the SRS-AW system with parametrization which stabilizes Kagome lattice. We confirmed the sequence of phases which was found in Ref. [47] and for the first time calculated the complete phase diagram. We studied in details the melting line of the low-density triangular and square phases. Both of these phases demonstrate two different melting scenarios with tricritical points at the maximum of the melting line. In the case of the low-density triangular phase the low-density branch of the melting line proceeds by the third scenario, while the high density one - via BKTHNY scenario. In the case of the square phase the situation is reversed: the low density branch proceeds via BKTHNY scenario, while the high-density one by the third scenario.

ACKNOWLEDGMENTS

This work was carried out using computing resources of the federal collective usage centre "Complex for simulation and data processing for mega-science facilities" at NRC "Kurchatov Institute", <http://ckp.nrcki.ru>, and supercomputers at Joint Supercomputer Center of the Russian Academy of Sciences (JSCC RAS). The work was supported by the Russian Science Foundation (Grant No 19-12-00092).

-
- [1] L.D. Landau, E.M. Lifshitz, Statistical Physics, Pergamon Press, Ltd., London, 1958, p. 482.
 - [2] N.D. Mermin, Phys. Rev. 176 (1968) 250.
 - [3] V. N. Ryzhov, E. E. Tareyeva, Yu. D. Fomin, and E. N. Tsiok, Phys. Usp. 60 857885 (2017).
 - [4] V.L. Berezinskii, Zh. Eksp. Teor. Fiz. 59 (1970) 907; Sov. Phys.JETP 32 (1970) 493.
 - [5] V.L. Berezinskii, Zh. Eksp. Teor. Fiz. 61 (1971) 1144; Sov. Phys.JETP 34 (1971) 610.
 - [6] J.M. Kosterlitz, D.J. Thouless, J. Phys. C 5 (1972) L124.
 - [7] J.M. Kosterlitz, D.J. Thouless, J. Phys. C 6 (1973) 1181.
 - [8] B. I. Halperin and D. R. Nelson, *Phys. Rev. Lett.*, 1978, **41**, 121.
 - [9] D. R. Nelson and B. I. Halperin, *Phys. Rev. B: Condens. Matter Mater. Phys.*, 1979, **19**, 2457.
 - [10] A. P. Young, *Phys. Rev. B: Condens. Matter Mater. Phys.*, 1979, **19**, 1855.
 - [11] E. P. Bernard and W. Krauth, Phys. Rev. Lett. 107, 155704 (2011).
 - [12] M. Engel, J. A. Anderson, Sh. C. Glotzer, M. Isobe, E. P. Bernard, and W. Krauth, Phys. Rev. E 87, 042134 (2013).
 - [13] S. C. Kapfer and W. Krauth, Phys. Rev. Lett. 114, 035702 (2015).
 - [14] A. K. Geim and K. S. Novoselov, Nature Materials 6, 183-191 (2007).

- [15] G. Algara-Siller, O. Lehtinen, F. C. Wang, R. R. Nair, U. Kaiser, H. A. Wu, A. K. Geim and I. V. Grigorieva, *Nature* 519, 443 (2015).
- [16] Jiong Zhao et al., *Science* 343, 1228 (2014).
- [17] N. Osterman, D. *Babič*, I. I. Poberaj, J. Dobnikar, and P. Zihlerl, *Phys. Rev. Lett.* 99, 248301 (2007).
- [18] W.L. Miller and A. Cacciuto, *Soft Matter* 7, 7552 (2011).
- [19] M. Zu, P. Tan, and N. Xu, *Nat. Comm.* 8, 2089 (2017).
- [20] Yu. D. Fomin, E. A. Gaiduk, E. N. Tsiok, and V. N. Ryzhov, *Mol. Phys.* doi.org/10.1080/00268976.2018.1464676
- [21] D.E. Dudalov, Yu.D. Fomin, E.N. Tsiok, and V.N. Ryzhov, *Journal of Physics: Conference Series* 510 (2014) 012016.
- [22] D. E. Dudalov, E. N. Tsiok, Yu. D. Fomin, and V. N. Ryzhov, *J. Chem. Phys.* 141, 18C522 (2014).
- [23] E. N. Tsiok, D. E. Dudalov, Yu. D. Fomin, and V. N. Ryzhov, *Phys. Rev. E* 92, 032110 (2015).
- [24] D.E. Dudalov, Yu.D. Fomin, E.N. Tsiok, and V.N. Ryzhov, *Soft Matter*, 10, 4966 (2014).
- [25] N. P. Kryuchkov, S. O. Yurchenko, Yu. D. Fomin, E. N. Tsiok, and V. N. Ryzhov, *Soft Matter* 14, 2152 (2018)
- [26] A. Jain, J. R. Errington and Th. M. Truskett, *Phys. Rev. X* 4, 031049 (2014).
- [27] W. D. Piñeros, M. Baldea, and Th. M. Truskett, *J. Chem. Phys.* 144, 084502 (2016).
- [28] W. D. Piñeros, M. Baldea, and Th. M. Truskett, *J. Chem. Phys.* 145, 054901 (2016).
- [29] M. Engel and H.-R. Trebin, *Phys. Rev. Lett.* 98, 225505 (2007).
- [30] T. Dotera, T. Oshiro, and P. Zihlerl, *Nature* 506, 208211 (2014).
- [31] H. Pattabhiraman and M. Dijkstra, *J. Chem. Phys.* 146, 114901 (2017).
- [32] P. G. Debenedetti, V. S. Raghavan and S. S. Borik, *J. of Phys. Chem.* 95, 4540 (1991).
- [33] Ryzhov V N, Tareyeva E E, Fomin Yu D, Tsiok E N, Complex phase diagrams of systems with isotropic potentials: results of computer simulation, 2020, *Phys. Usp.*, *accepted*; DOI : 10.3367/UFNe.2018.04.038417
- [34] Yu. D. Fomin, N. V. Gribova, V. N. Ryzhov, S. M. Stishov, and Daan Frenkel, *J. Chem. Phys.* 129, 064512 (2008).
- [35] Fomin Yu D, Tsiok E N, and Ryzhov V N, 2011, *J. Chem. Phys.* 135, 234502
- [36] Fomin Yu D and Ryzhov V N, 2011, *Physics Letters A* 375, 21812184
- [37] Fomin Yu D, Tsiok E N, and Ryzhov V N, 2013, *Eur. Phys. J. Special Topics* 216, 165173
- [38] Fomin Yu D, Tsiok E N, and Ryzhov V. N, 2011, *J. Chem. Phys.* 135, 124512
- [39] Yu. D. Fomin, E. N. Tsiok, and V. N. Ryzhov, *J. Chem. Phys.* 134, 044523 (2011).
- [40] Yu. D. Fomin, E. N. Tsiok, and V. N. Ryzhov, *Phys. Rev. E* 87, 042122 (2013).
- [41] Yu. D. Fomin, E. N. Tsiok, and V. N. Ryzhov, *Eur. Phys. J. Special Topics* 216, 165173 (2013).
- [42] Yu. D. Fomin, E. N. Tsiok, and V. N. Ryzhov, *J. Chem. Phys.* 135, 124512 (2011).
- [43] E. Marcotte, F. H. Stillinger, and S. Torquato, *J. Chem. Phys.* 134, 164105 (2011).
- [44] A. Jain, J. R. Errington and Th. M. Truskett, *Soft Matter*, 9, 3866 (2013).
- [45] W. D. Pineros, M. Baldea, and Th. M. Truskett, *J. Chem. Phys.* 144, 084502 (2016).
- [46] W. D. Pineros, M. Baldea, and Th. M. Truskett, *J. Chem. Phys.* 145, 054901 (2016).
- [47] L. Nowack and S. A. Rice, *J. Chem. Phys.* 151, 244504 (2019)
- [48] E. N. Tsiok, E. A. Gaiduk, Yu. D. Fomin and V. N. Ryzhov, *Soft Matter*, 16, 3962-3972 (2020)
- [49] Juan J. Alonso and Julio F. Fernandez, *Phys. Rev. E* 59, 2659 (1999).
- [50] E. N. Tsiok, Y. D. Fomin, V. N. Ryzhov, *Physica A*, 2018, **490**, 819.
- [51] E. N. Tsiok, D. E. Dudalov, Yu. D. Fomin, and V. N. Ryzhov, *Phys. Rev. E: Stat. Phys., Plasmas, Fluids, Relat. Interdiscip. Top.*, 2015, **92**, 032110.
- [52] <http://lammmps.sandia.gov/>
- [53] Yu.D. Fomin, E.N. Tsiok, V.N. Ryzhov, *Physica A* 527, 121401 (2019).
- [54] Q. Chen, S. Chul Bae, and S. Granick, *Nature* 469, 381384 (2011).

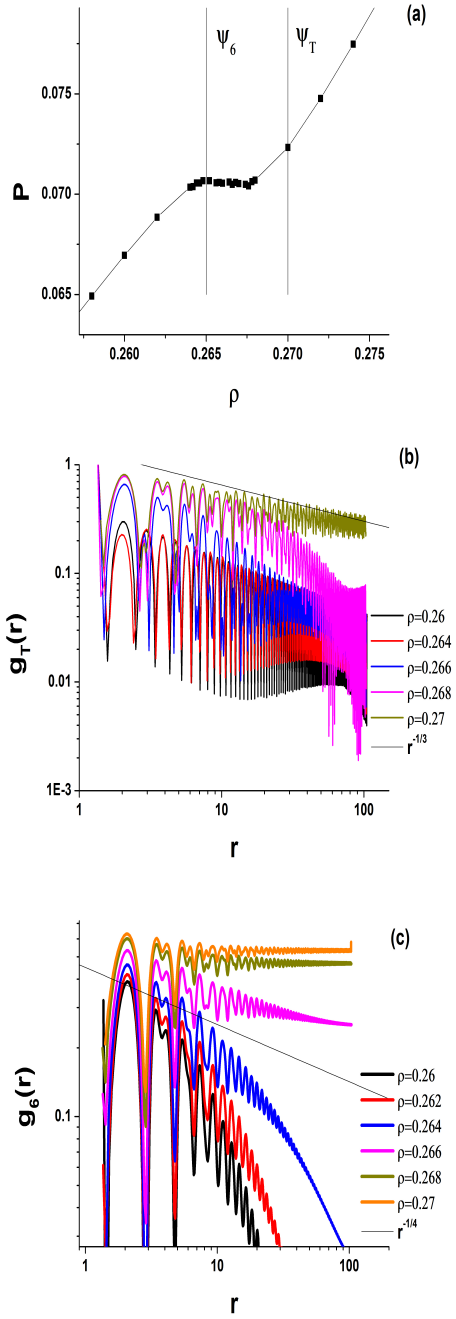


FIG. 4: (a) Equation of state of the system at $T = 0.02$ in the region of the low-density branch of the melting line of the low-density triangular crystal. (b) TCF in the same region. (c) OCF in the same region. The vertical lines at panel (a) show the limit of stability of the crystal with respect to the hexatic phase (ψ_T) and the limit of stability of the hexatic phase with respect to the isotropic liquids (ψ_6).

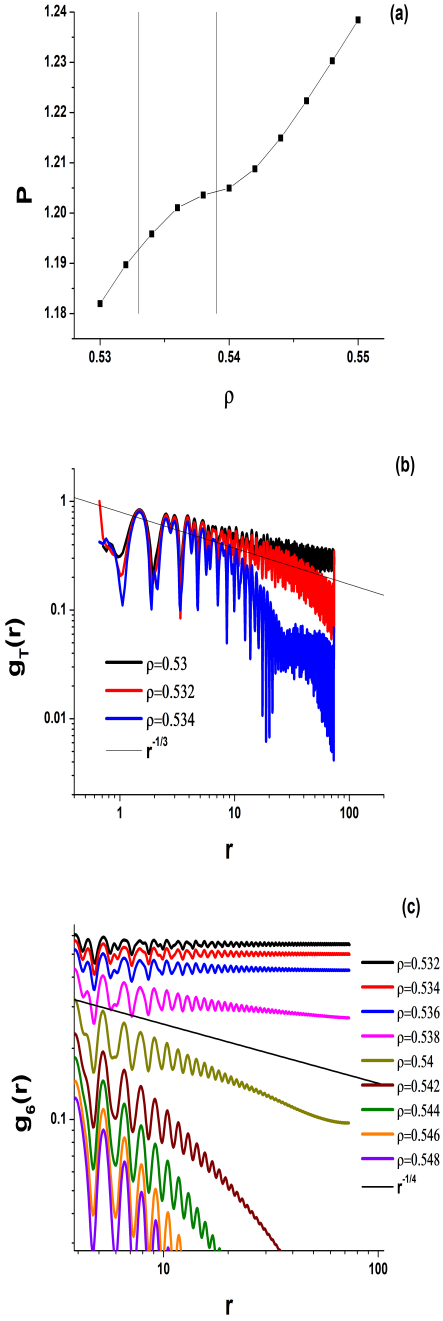


FIG. 5: (a) Equation of state of the system at $T = 0.02$ in the region of the high-density branch of the melting line of the low-density triangular crystal. (b) TCF in the same region. (c) OCF in the same region. The vertical lines at panel (a) show the limit of stability of the crystal with respect to the hexatic phase (ψ_T) and the limit of stability of the hexatic phase with respect to the isotropic liquids (ψ_6).

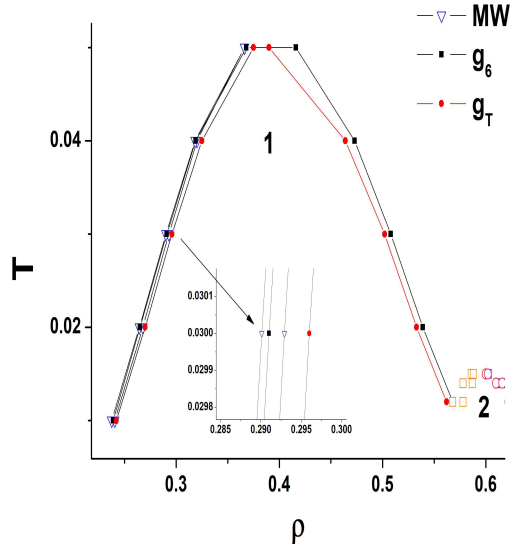


FIG. 6: A part of the phase diagram in the vicinity of the low-density triangular phase. The line MW means the melting phase. The line MW means the melting points obtained from the Mayer-Wood loop. the lines g_6 and g_T mark the limits of stability of the hexatic phase with respect to liquid and the crystal with respect to the hexatic phase obtained from OCF and TCF respectively. The inset enlarges the left branch at $T = 0.03$. From this inset one can see that going from the higher density to the lower through the melting line firstly the crystal transforms into hexatic phase and then the hexatic phase transforms into liquid through the first order transition, because the point of the g_6 line is in between of the MW line points.

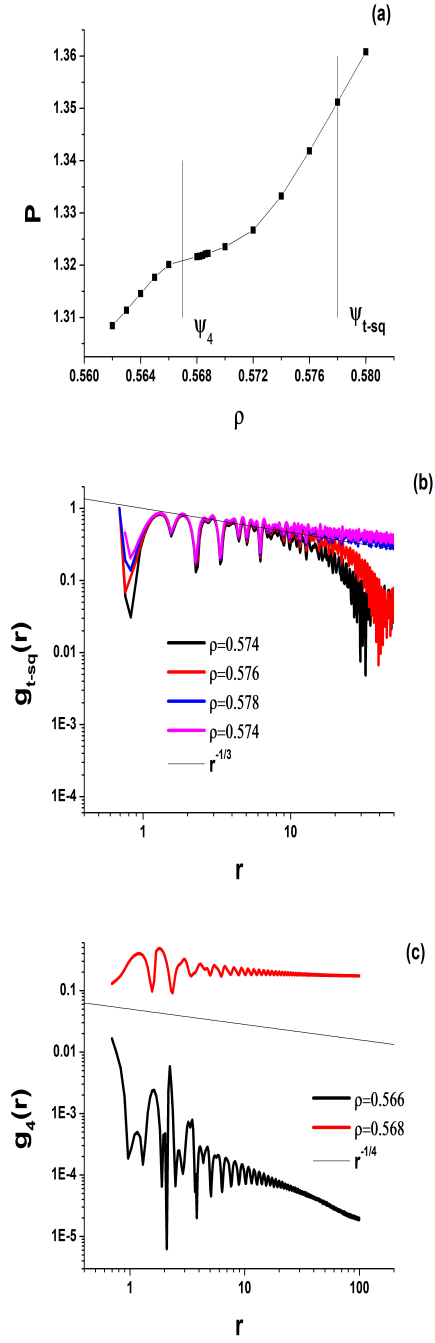


FIG. 7: (a) Equation of state of the system at $T = 0.012$ in the region of the low-density branch of the melting line of the square crystal. (b) TCF in the same region. (c) OCF in the same region. The vertical lines at panel (a) show the limit of stability of the crystal with respect to the tetratic phase (ψ_{t-sq}) and the limit of stability of the tetratic phase with respect to the isotropic liquids (ψ_4).

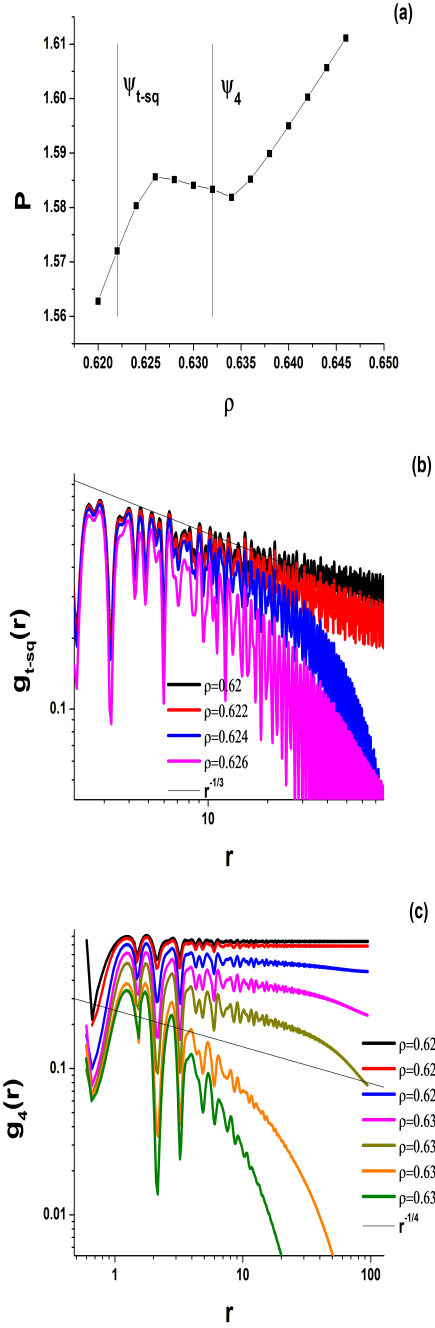


FIG. 8: (a) Equation of state of the system at $T = 0.012$ in the region of the high-density branch of the melting line of the square crystal. (b) TCF in the same region. (c) OCF in the same region. The vertical lines at panel (a) show the limit of stability of the crystal with respect to the tetratic phase (ψ_{t-sq}) and the limit of stability of the tetratic phase with respect to the isotropic liquids (ψ_4).

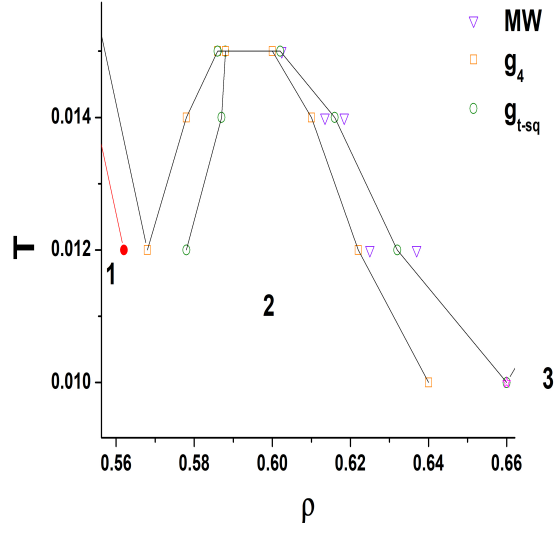


FIG. 9: A part of the phase diagram in the vicinity of the square crystal. The line MW means the melting points obtained from the Mayer-Wood loop. The lines g_4 and g_{t-sq} mark the limits of stability of the hexatic phase with respect to liquid and the crystal with respect to the hexatic phase obtained from OCF and TCF respectively.